Electronic Supplementary Material (ESI) for RSC Advances.

Effect of Mg2+/Li+ mixed electrolytes on a rechargeable hybrid battery with Li4Ti5O12 cathode and Mg anode

Qi Miao, Yanna NuLi,* Nan Wang, Jun Yang, Jiulin Wang and Shin-ichi Hirano

Supporting Information

Experimental

Electrolyte preparation

The preparation was conducted in an argon-filled glove box (Mbraun, Unilab, Germany) with H_2O and O_2 below 2 ppm. 0.5 mol L^{-1} $Mg(BH_4)_2$+1.5 mol L^{-1} $LiBH_4$/TG electrolyte was prepared by dissolving the predetermined amount of $Mg(BH_4)_2$ (Sigma-Aldrich, 95%) and $LiBH_4$ (J&K Scientific, 95%) in tetraglyme (TG) (from Aladdin, and further dried using a 3 Å molecular sieve) under stirring at 90^{o}C for at least 12 hours. 0.4 mol L^{-1} $(PhMgCl)_2$-$AlCl_3$+1.5 mol L^{-1} $LiBH_4$/THF electrolyte was prepared by dissolving the predetermined amount of PhMgCl (Sigma-Aldrich, 95%), $AlCl_3$ (Alfa Aesar, 99.999%) and $LiBH_4$ (J&K Scientific, 95%) in tetrahydrofuran (THF) (from Aladdin, and further dried using a 3 Å molecular sieve) under stirring for at least 24 hours.

LTO/G material preparation

LTO/G composite was prepared by ball-milling $Li_4Ti_5O_{12}$ (LTO) powder (Shenzhen Tianjiao Technology Co., Ltd.) and graphene (G) powder (Deyang Carbonene Technology Co., Ltd.) at a weight ratio of 8:2. The mixture and appropriate NMP were added into a 50mL agate holding tank under vigorous stirring for 4 hours with 500r/min rotate speed to form a uniform mixture. Afterwards, the LTO/G composite was obtained after drying at 80^{o}C for at least 12 hours under vacuum to remove the solvent.

Material Characterization

X-ray diffraction (XRD) measurements were performed on a Rigaku diffractometer D/MAX-2200/PC equipped with Cu Kα radiation (λ = 0.15418 nm). Textural characterizations were conducted using scanning electron microscopy (SEM) on a JEOL field-emission microscope (JSM-7401F) and transmission electron microscopy (TEM) on a JEOL high-resolution electron microscope (JEM-2010). Raman spectra were collected at room temperature with a DXR Raman microscope (Thermo Scientific) using a HeNe laser with a wavelength of 532 nm as the excitation source. The specific conductivity of the electrolytes was measured using a DDB-303A conductivity meter (INESA INSTRUMENT).

The morphology of particle and electrode surface after rate cycles were observed using scanning electron microscopy (SEM) on a JEOL field-emission microscope (JSM-7401F). The Energy Dispersive X-Ray (EDX) measurements for electrodes with 70% PVDF+30% Super-P on SS substrate scanned to different cut-off potentials by linear sweep voltammetry (LSV) were conducted using scanning electron microscopy (SEM) on a JEOL field-emission microscope (JSM-7401F). Before the measurement, the electrode after the cycle was washed in an argon-filled glove box (Mbraun, Unilab, Germany) with THF solvent to remove soluble residue and then transferred out of the box and kept without exposure to the atmosphere.

Electrochemical Measurements

Electrode slurry was prepared by mixing 80 wt.% cathode material, 10 wt.% super-P carbon powder (Timcal) and 10 wt.% poly(vinylidene fluoride) (PVDF) dissolved in N-methyl-2-pyrrolidinone. The electrode was formed by coating the slurry onto stainless steel foil current collector, drying at 80 ^{o}C for 1 hour, pressing at 2 MPa, and drying again at 80 ^{o}C for at least 12 hours under vacuum. The electrode, with a diameter of Φ12 mm, contains 0.4-0.6 mg active material, and the typical thickness of the active layer is 100 μm. Electrochemical behavior of LTO|Li^+, Mg^{2+}|Mg was examined via CR2016 coin cells with a magnesium counter electrode, an Entek PE membrane separator and 0.5 mol L^{-1} $Mg(BH_4)_2$+1.5 mol L^{-1} $LiBH_4$/TG or 0.4 mol L^{-1} $(PhMgCl)_2$-$AlCl_3$+1.5 mol L^{-1} $LiBH_4$/THF electrolytes. The cells were assembled in an argon-filled glove box. As a comparison, electrochemical behavior of LTO|Li^+|Li cell was examined with a lithium counter electrode, and 1.5 mol L^{-1} $LiBH_4$/TG or 1.5 mol L^{-1} $LiBH_4$/THF electrolytes; LTO|Mg^{2+}|Mg with a magnesium counter electrode, and 0.5 mol L^{-1} $Mg(BH_4)_2$/TG or 0.5 mol L^{-1} $Mg(BH_4)_2$/THF electrolytes. Cyclic voltammetry measurements were performed on a CHI650C Electrochemical Workstation (Shanghai, China). Electrochemical impendence spectra

(EIS) were conducted on Autolab PGSTAT302N Electrochemical Workstation (Switherland). Galvanostatic discharge-charge measurements were conducted at ambient temperature on a Land battery measurement system (Wuhan, China) with the cut-off voltages of 0.3/1.7 V *vs*. Mg and 1.0/2.5V *vs*. Li.

Table S1 The 1st and 20th discharge and charge capacities, coulombic efficiencies and cycling stability of LTO and LTO/G with different weight ratios at 0.1 C. The electrolyte is 0.4 mol L^{-1} $(PhMgCl)_2$-$AlCl_3$+1.5 mol L^{-1} $LiBH_4$/THF.

	1st			20th		
	discharge efficiency (mAh g^{-1})	charge (mAh g^{-1})	(%)	discharge (mAh g^{-1})	charge stability (mAh g^{-1})	cycling (%)
LTO	166.8	165.5	99.2	156.8	157.4	94.0
LTO/G (80:20)	169.3	184.2	108.8	164.8	165.4	97.3
LTO/G (70:30)	171.8	191.0	111.2	152.8	152.3	88.9
LTO/G (60:40)	174.4	209.9	120.4	146.3	147.5	83.9

Table S2 The Energy Dispersive X-Ray (EDX) results for electrodes with 70% PVDF+30% Super-P on SS substrate scanned to different cut-off potentials by linear sweep voltammetry (LSV). The electrolyte is 0.4 mol L^{-1} $(PhMgCl)_2$-$AlCl_3$+1.5 mol L^{-1} $LiBH_4$/THF.

	before scanning		1.7V		2.5V		3.0V	
	Wt%	At%	Wt%	At%	Wt%	At%	Wt %	At %
C	69.42	80.26	67.31	78.95	66.53	78.14	64.48	76.68
F	26.62 19.46		26.69 19.79		28.30 21.01		29.55 22.21	

Table S3 Fitted resistance values of the EIS spectra shown in Fig. 3c.

	R_s (Ω mg^{-1})	R_{ct} (Ω mg^{-1})
LTO	18.66	89.97
LTO/G (80:20)	23.63	50.63

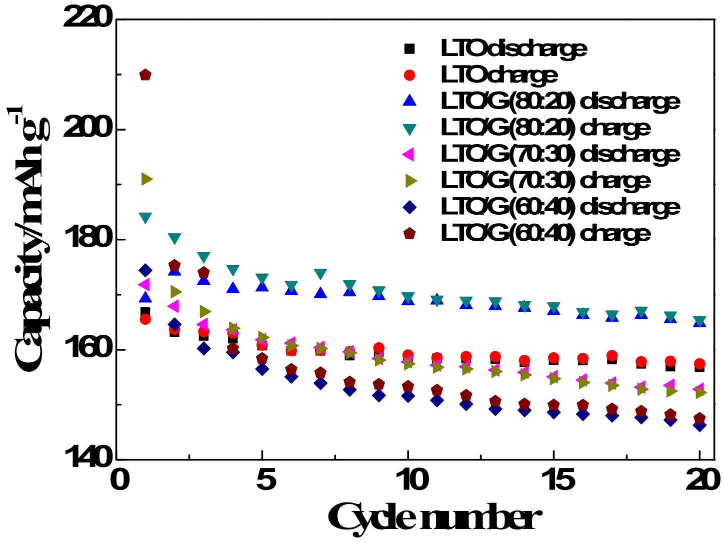

Figure S1a. The discharging-charging cycling performance of LTO and LTO/G with different weight ratios at 0.1 C. The electrolyte is 0.4 mol L^{-1} $(PhMgCl)_2$-$AlCl_3$+1.5 mol L^{-1} $LiBH_4$/THF.

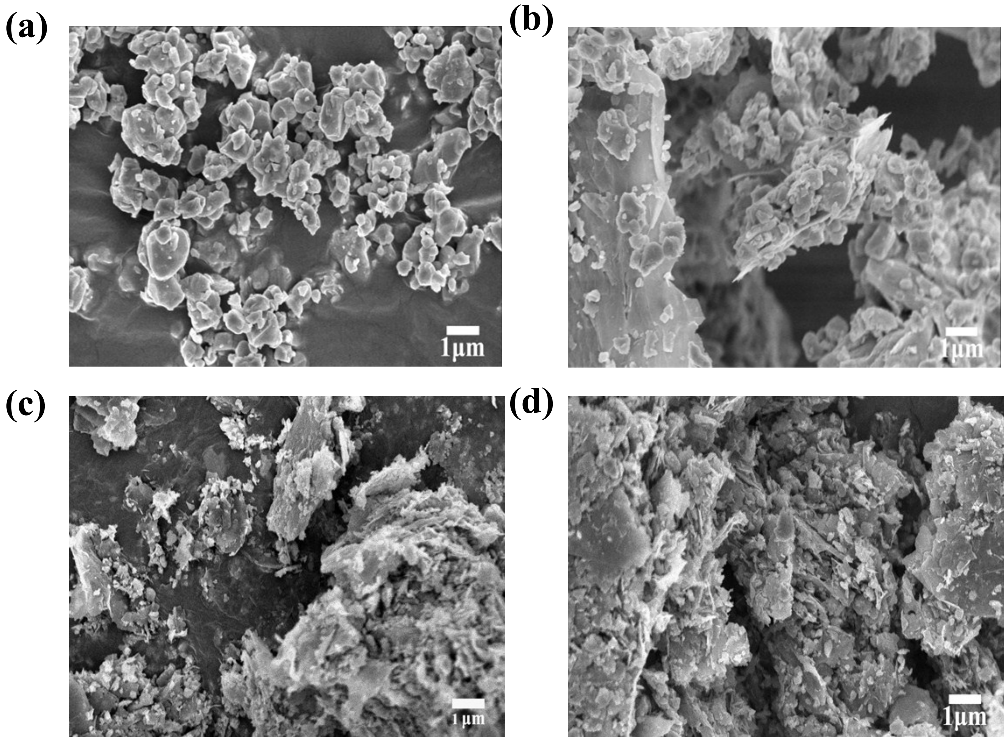

Figure S1b. SEM images of LTO (a) and LTO/G composite with different weight ratios of 80:20 (b), 70:30 (c) and 60:40 (d).

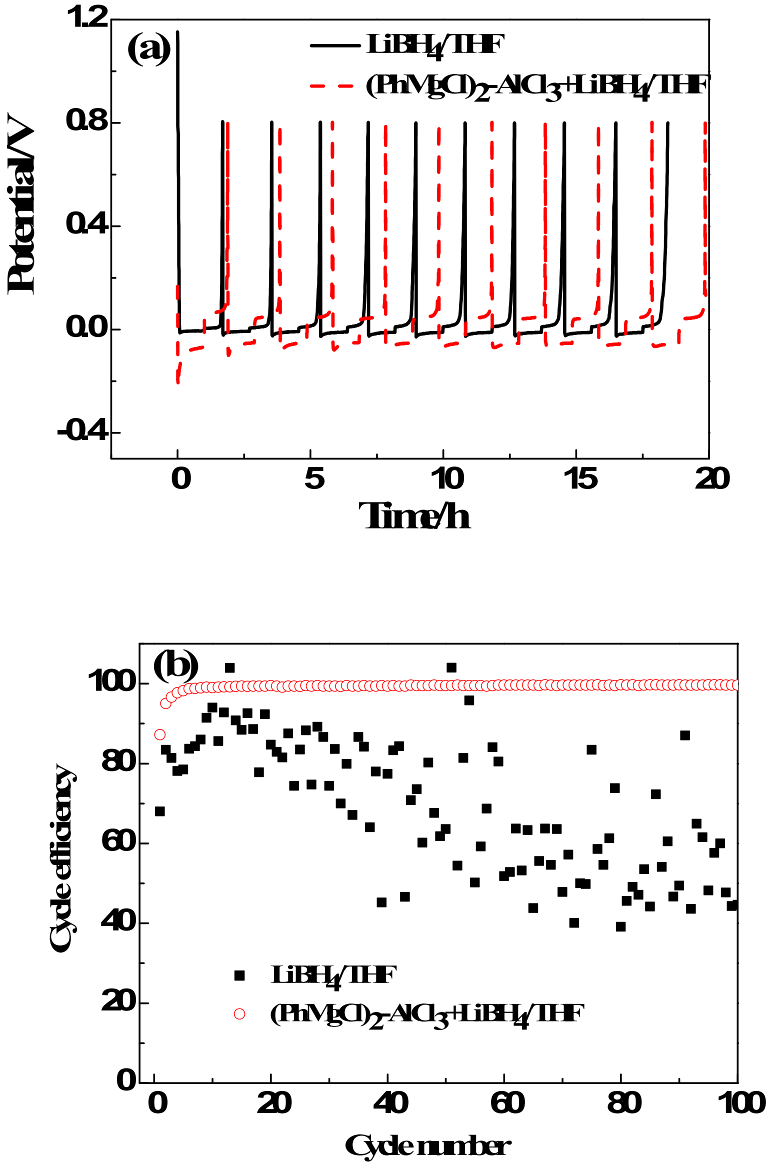

Figure S2. The deposition-dissolution cycling curves (a), and the corresponding efficiency (b) of Li deposition-dissolution from 1.5 mol L^{-1} $LiBH_4$/THF and Mg deposition-dissolution from 0.4 mol L^{-1} $(PhMgCl)_2$-$AlCl_3$+1.5 mol L^{-1} $LiBH_4$/THF on SS substrate.

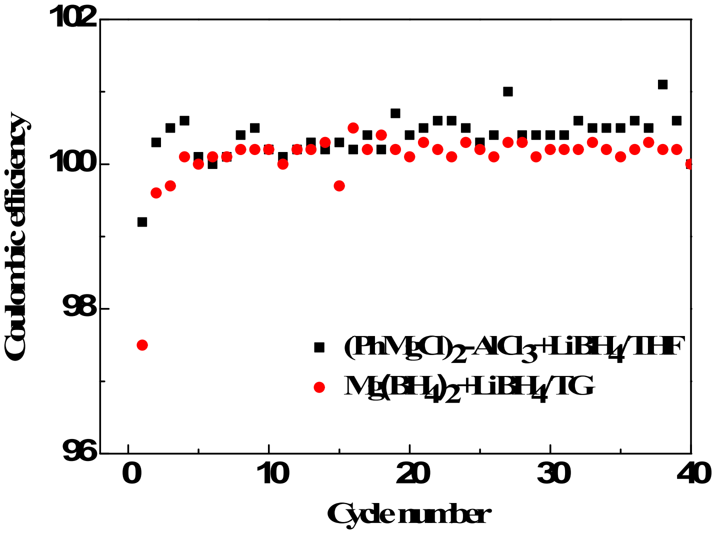

Figure S3. Coulombic efficiency of discharge-charge cycling for LTO|Li^+, Mg^{2+}|Mg cells with 0.4 mol L^{-1} $(PhMgCl)_2$-$AlCl_3$+1.5 mol L^{-1} $LiBH_4$/THF and 0.5 mol L^{-1} $Mg(BH_4)_2$+ 1.5 mol L^{-1} $LiBH_4$/TG at 0.1 C.

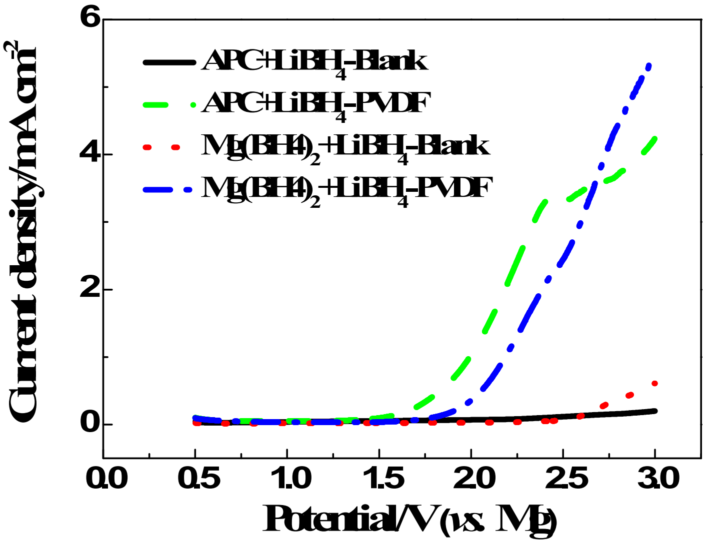

Figure S4. The liner sweep voltammetry (LSV) of 0.5 mol L^{-1} $Mg(BH_4)_2$+1.5 mol L^{-1} $LiBH_4$/TG and 0.4 mol L^{-1} $(PhMgCl)_2$-$AlCl_3$+1.5 mol L^{-1} $LiBH_4$/THF electrolytes on blank SS substrate and SS substrate with 70% PVDF+30% Super-P. The scan rate is 10 mV s^{-1}.

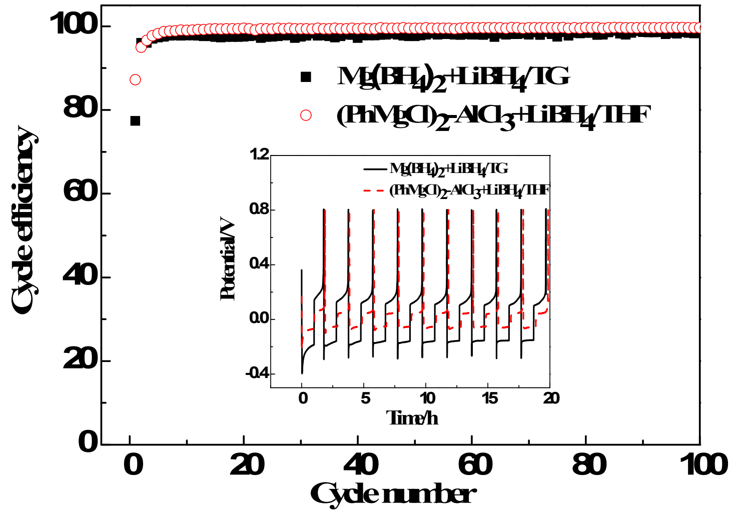

Figure S5. The cycling efficiency of Mg deposition-dissolution on SS substrate from 0.5 mol L^{-1} $Mg(BH_4)_2$+1.5 mol L^{-1} $LiBH_4$/TG and 0.4 mol L^{-1} $(PhMgCl)_2$-$AlCl_3$+1.5 mol L^{-1} $LiBH_4$/THF electrolytes, inset is the deposition-dissolution cycling curves.

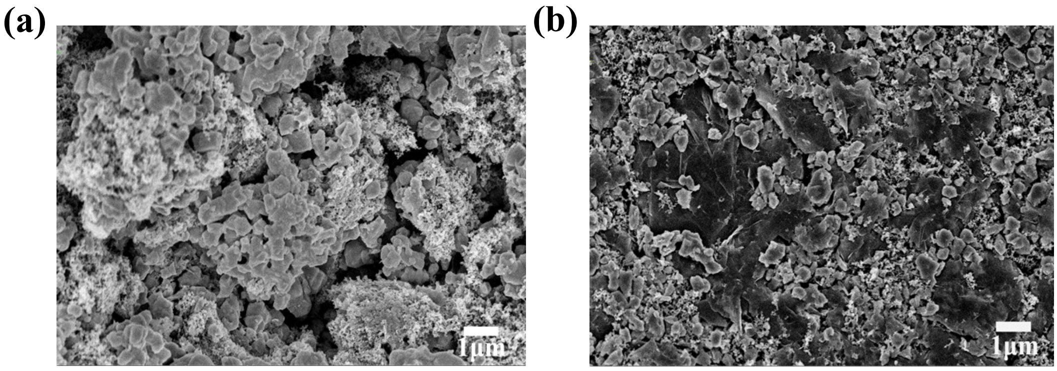

Figure S6. SEM images of the electrode surface of LTO (a) and LTO/G (b) after rate cycling. The electrolyte is 0.4 mol L^{-1} $(PhMgCl)_2$-$AlCl_3$+1.5 mol L^{-1} $LiBH_4$/TG.

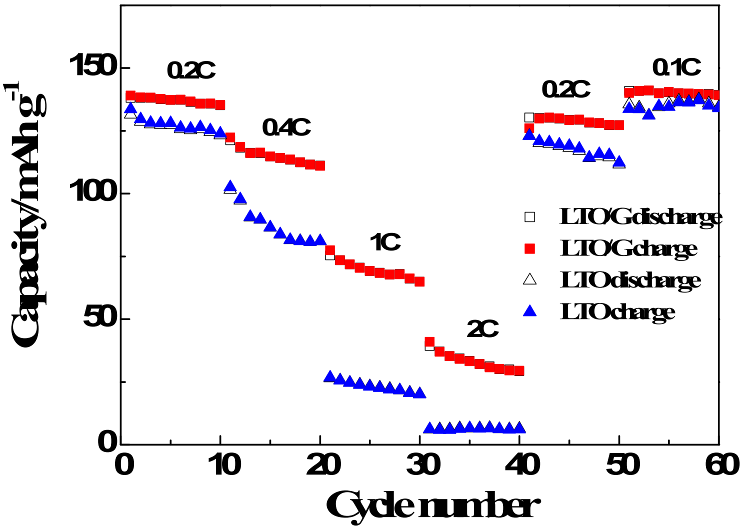

Figure S7. Rate capability of the cells of LTO|Li^+, Mg^{2+}|Mg and LTO/G|Li^+, Mg^{2+}|Mg. The electrolyte is 0.5 mol L^{-1} $Mg(BH_4)_2$+1.5 mol L^{-1} $LiBH_4$/TG.